

New Insights into the Growth and Transformation of Vesicles: A Free-Flow Electrophoresis Study

Tereza Pereira de Souza,^{†,‡} Martin Holzer,[‡] Pasquale Stano,[§] Frank Steiniger,^{||} Sylvio May,[⊥] Rolf Schubert,[‡] Alfred Fahr,^{*,†} and Pier Luigi Luisi^{*,§}

[†]Institut für Pharmazie, Friedrich Schiller Universität Jena; Lessingstrasse 8, D-07743 Jena, Germany

[‡]Department of Pharmaceutical Technology and Biopharmacy, Albert Ludwigs University Freiburg, D-79104 Freiburg, Germany

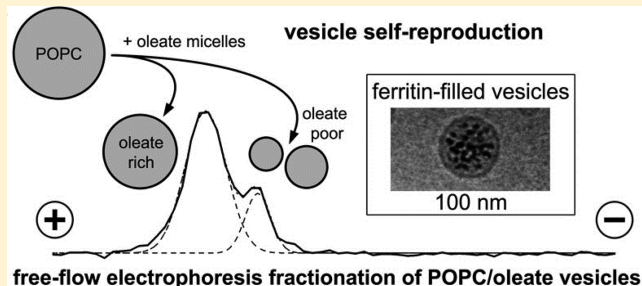
[§]Science Department, Roma Tre University; Viale G. Marconi 446, I-00146 Rome, Italy

^{||}Elektronenmikroskopisches Zentrum, Friedrich Schiller Universität Jena; Ziegelmühlenweg 1, D-07743 Jena, Germany

[⊥]Department of Physics, North Dakota State University, Fargo North Dakota 58108-6050, United States

Supporting Information

ABSTRACT: The spontaneous formation of lipid vesicles, in particular fatty acid vesicles, is considered an important physical process at the roots of cellular life. It has been demonstrated previously that the addition of fatty acid micelles to preformed vesicles induces vesicle self-reproduction by a growth-division mechanism. Despite multiple experimental efforts, it remains unresolved how vesicles rearrange upon the addition of fresh membrane-forming compounds, and whether solutes that are initially encapsulated inside the mother vesicles are evenly redistributed among the daughter ones. Here we investigate the growth-division of 1-palmitoyl-2-oleoyl-*sn*-glycero-3-phosphatidylcholine (POPC) vesicles, which, following the addition of oleate micelles, form mixed oleate/POPC vesicles. Our approach is based on free-flow electrophoresis (FFE) and cryogenic transmission electron microscopy (cryo-TEM). Two new features emerge from this study. FFE analysis unexpectedly reveals that the uptake of oleate micelles by POPC vesicles follows two different pathways depending on the micelles/vesicles ratio. At low oleate molar fractions (<0.35), plain incorporation of oleate into pre-existing POPC vesicles is our dominant observation. In contrast, oleate-rich and oleate-poor daughter vesicles are generated from parent POPC vesicles when the oleate molar fraction exceeds 0.35. Cryo-TEM reveals that when ferritin-filled vesicles grow and divide, some vesicles contain ferritin at increased concentrations, others are empty. Intriguingly, in some cases, ferritin appears to be highly concentrated inside the vesicles. These observations imply a specific redistribution (partitioning) of encapsulated solutes among nascent vesicles during the growth-division steps. We have interpreted our observations by assuming that freshly added oleate molecules are taken-up preferentially (cooperatively) by oleate-rich membrane regions that form spontaneously in POPC/oleate vesicles when a certain threshold (oleate molar fraction ca. 0.35) is surpassed. The proposed cooperative mechanism could be based on differential microscopic constants for oleate/oleic acid dynamics in oleate-rich and oleate-poor membrane regions, which eventually generate populations of oleate-rich and oleate-poor vesicles.



1. INTRODUCTION

Autopoietic “self-reproduction” of micelles¹ and vesicles² is being considered as a realistic model of primitive cell proliferation (see the review³). The relevance of autopoietic self-reproduction has become widely recognized within the origin-of-life community⁴ and is now being integrated into the conceptual scenarios and experimental approaches that rationalize the origin of living cells.^{5–10}

The autopoietic self-reproduction of fatty acid vesicles can be accomplished by feeding preformed vesicles with an insoluble membrane precursor, fatty acid anhydride, which is taken up by vesicles and hydrolyzed *in situ*. Oleic acid/oleate vesicles (shortly “oleate vesicles”) and oleic anhydride have been used in these experiments. As a result of this process, the vesicles

grow, reach an unstable state, and eventually divide.² Similar results can be obtained by substituting the oleic anhydride by oleate micelles.

We have reported earlier that the addition of oleate micelles to oleate vesicles or 1-palmitoyl-2-oleoyl-*sn*-glycero-3-phosphatidylcholine (POPC) vesicles results in vesicle self-reproduction, and that the preformed vesicles exert a “matrix effect” on the size of the newly formed ones.^{5–7,11,12}

In particular, when oleate micelles (stable only at pH higher than about 10) are added to plain buffer (pH 8.5), a slow

Received: May 27, 2015

Revised: August 12, 2015

Published: September 4, 2015



ACS Publications

© 2015 American Chemical Society

12212

DOI: 10.1021/acs.jpcb.5b05057
J. Phys. Chem. B 2015, 119, 12212–12223

micelle-to-vesicle transition is observed owing to oleate protonation. In contrast, if preformed oleate vesicles or POPC vesicles are already present in buffer, at pH = 8.5, rapid formation of new vesicles occurs. These different behaviors are illustrated in Figure 1, showing the typical

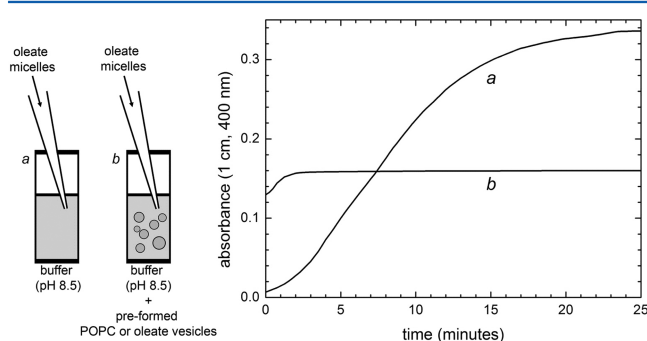


Figure 1. Oleate micelle-to-vesicle transformation in the absence (a) or in the presence (b) of preformed POPC vesicles. Oleate micelles were added to 200 mM bicine buffer (pH 8.5) and the variation of absorbance (400 nm), indicating the formation of vesicles, was followed in time. A sigmoidal profile, with $t_{1/2}$ of around 7 min, and plateau value of about 0.34 was obtained. By contrast, when an equimolar amount of extruded POPC vesicles was present (2 mM), the micelle growth reached a final (but lower) value quite rapidly ($t_{1/2}$ ca. 1 min). Oleate micelles clearly interact with preformed POPC vesicles. Data are interpreted as evidence of oleate uptake by POPC vesicles, followed by a growth-division mechanism. The right-hand side plot has been reproduced from ref 7. Copyright 2003 American Chemical Society.

kinetics of the two processes. Clearly, micelles interact with preformed vesicles. Oleate molecules are taken up by preformed vesicles, which grow in size owing to the incorporation of the added oleate into their membrane. In most cases the growing vesicles become structurally unstable and thus divide, giving rise to two (or more) daughter vesicles (Figure SI.1). Note that this fast process competes with the *de novo* vesicle formation from micelles, which occurs simultaneously. It has been shown by dynamic light scattering that the vesicles formed by the growth–division sequence have an average size that mimics that of the preformed vesicles (hence the name “matrix effect”).^{5–7} Electron microscopy images suggest possible intermediate structures just before vesicle division.¹³ Recent studies have also pointed out the importance of the micelle addition rate,¹⁴ the role of buffer (membrane-permeable versus membrane-impermeable species) when similar processes are induced in giant vesicles,⁸ and the existence of evagination/invagination mechanisms.¹⁵

Despite these advancements, most of the physics responsible for vesicle self-reproduction through growth and division remains unexplained.³ This is due to the difficulty of monitoring structural changes of vesicles, especially when conventional (<μm) vesicles are studied. As a result, we still lack quantitative models for fatty acid uptake, membrane growth, deformation, and division. Moreover, the question, how encapsulated solutes are distributed among daughter vesicles, has not been addressed previously.

Fatty acid vesicles are negatively charged due to the presence of carboxylate moieties. This suggests to employ free-flow electrophoresis (FFE) to study vesicle self-reproduction and the matrix effect. FFE is an analytical and preparative electrophoretic technique introduced in the 1960s and applied

by De Cuyper and collaborators to study lipid transfer among vesicles;^{16,17} but it has never been used for studying vesicles based on fatty acids. Charged vesicles are suitable objects for FFE separation. Lipid vesicles, when injected in the FFE apparatus, are transported from the injection site to the collecting slot by a continuous solvent flow. On their path, uncharged vesicles travel undisturbed, whereas ionic vesicles are deflected toward the electrodes (located on the sides of the apparatus) according to their charges, and can be collected in multiple fractions (a schematic drawing of the instrument is shown in Figure SI.2). FFE is a versatile technique that allows separation and analysis of vesicles according to the charge they contain. In the context of vesicle self-reproduction, FFE becomes particularly convenient when negatively charged oleate micelles are added to zwitterionic POPC vesicles, because it is expected that the charge density of the vesicle membrane reflects the extent of oleate uptake.

In this work, we study the vesicle self-reproduction process and the matrix effect based on oleate micelle addition to POPC vesicles employing FFE separation and cryo-transmission electron microscopy (cryo-TEM). We show that two different kinetic pathways emerge, depending on the amount of added oleate, and we demonstrate that the chemical composition of daughter vesicles can vary substantially within a population. We also studied the self-reproduction of ferritin-containing POPC vesicles in order to follow the fate of entrapped solutes during vesicle self-reproduction, revealing intriguing anomalies of solutes redistribution among daughter vesicles.

2. EXPERIMENTAL SECTION

Vesicle Preparation. (a) POPC vesicles (60 mM) were prepared by the thin film hydration method. The appropriate amount of POPC (Avanti Polar Lipids) was first dissolved in chloroform and poured into a round-bottom flask. The solvent was removed under reduced pressure in a Rotavapor (Buchi) apparatus and further dried overnight in high vacuum. The resulting thin POPC film was hydrated with 200 mM bicine buffer, sodium salt (pH 8.5) (Sigma-Aldrich). Vesicles were then homogenized to the desired size (e.g., diameter 100 nm) by extrusion (20 times) through two stacked polycarbonate membranes (Whatman Nuclepore) using a Liposofast apparatus (Avestin). The stock POPC vesicles suspension was diluted to the desired concentration with 200 mM bicine buffer. (b) Ferritin-containing POPC vesicles (40 mM) were prepared by the reverse phase evaporation method.¹⁸ The appropriate amount of POPC was first dissolved in diethyl ether, to obtain a 16 mM POPC solution, and poured into a round-bottom flask. Then, 1 mL of a horse spleen ferritin solution (60 μM) (Sigma-Aldrich code F4503, MW 680 kDa, purified by dialysis and then lyophilized) in 200 mM bicine buffer, sodium salt (pH 8.5) was injected into 5 mL of the POPC solution to form a water-in-oil emulsion (by vortexing and short bath-sonication). After removal of the apolar phase under reduced pressure in a Rotavapor apparatus, typically, a gel was obtained, which was then diluted with buffer (1 mL) and transformed into vesicles by vigorous vortexing. The vesicles thus obtained (2 mL) where first freed from the last traces of diethyl ether *in vacuo*, then extruded as described above (diameter: 100 nm), and the free ferritin was removed by size exclusion chromatography. To this end, 200 μL of the ferritin-containing extruded POPC vesicles were applied on a homemade Sepharose 4B (Amersham) column (30 cm length × 1 cm i.d.) operating at about 0.2 mL/min buffer flow rate).

Purified vesicles were collected as turbid fractions and concentrated by centrifugation.

Addition of Oleate Micelles to Preformed POPC Vesicles.

Sodium oleate micelles were freshly prepared before each experiment by solubilizing sodium oleate (Sigma-Aldrich, code O7501) in ultrapure water. After vortexing and bath sonication (30 s), a transparent solution was obtained. The micelles, at a typical concentration of 200 mM, were added to POPC vesicles using a standard micropipet and mixed by pipetting up and down. The micelles were added to POPC vesicles within a short time (ca. 0.5 s). The final sodium oleate concentration was 40 mM, while the POPC concentration was varied in order to obtain different oleate/POPC molar ratios. For example, when $x_{OL} = 0.9$, [oleate] = 40 mM, [POPC] = 4.44 mM; when $x_{OL} = 0.5$, [oleate] = 40 mM, [POPC] = 40 mM; and so on.

Free-Flow Electrophoresis. An Octopus PZE (Weber FFE, Kirchheim, Germany) device with the separation chamber in the upright position was used in all FFE separations (see Figure SI.2). Within the chamber, a thin laminar film of bicine buffer (200 mM bicine, sodium salt, pH 8.5) was flowing upward at a rate of 2.5 mL/min. The dimensions of the resulting separation volume were 500 × 100 × 0.50 mm (height × width × depth) and the chamber was kept at 15 °C. The same bicine buffer was running through the electrode channels, which were separated from the chamber by a nonion-selective membrane. An electrical field of 45 V/cm perpendicular to the running buffer and samples was applied. After starting the voltage supply, a stabilization period of 60 min was required to achieve a constant current of approximately 400 mA.

Into the flowing bicine buffer, 70 μL of undiluted vesicle sample (prepared as specified above) were injected at a rate of 8 μL/min. Injection was done near the cathode (facing fraction no. 79) and the samples were then deflected in the electrical field toward the anode while traveling through the separation chamber. At the outlet of the chamber, the flow was collected in 96 fractions and lipid-containing fractions were identified as described below. The average pH measured in all fractions over a typical separation run time was 8.66 ± 0.02.

DPH-Based Fluorimetric Vesicle Detection. A diphenylhexatriene (DPH)/Brij-35 reagent was prepared by mixing 1.0 mL of an 11.5 mM stock solution of polyoxyethylene-23-laurylether (Brij-35, Sigma-Aldrich) in purified water with 230 μL of a 30 mM stock solution of DPH (Fluka) in tetrahydrofuran and adding purified water to obtain a final volume of 100 mL. The dispersion was then treated in an ultrasonic bath for 15 min and used within 1 day. Lipid-containing fractions were identified by mixing 100 μL of each FFE fraction with 100 μL of the reagent. After a 10 min incubation period at room temperature, the fluorescence at 460 nm was measured in a plate reader (FluoroCount, Canberra-Packard, Dreieich, Germany) using an excitation wavelength of 360 nm.¹⁹ Only vesicle-containing fractions gave rise to a significant fluorescence signal (above background), due to the intercalation of DPH in the lipid membrane. Electropherograms are presented as plots of DPH fluorescence intensity (in arbitrary units, a.u.) against fraction number.

Quantitation of Lipids by HPLC. The chemical composition of each fraction derived from the FFE separation was determined by HPLC. Sodium oleate and POPC can be separated on an XBridge C₁₈ 3.5 μm column (150 mm × 3 mm) from Waters, operating at 35 °C with a flow rate of 1.0 mL/min. The mobile phase was changed according to the

following linear gradient method (A, water/acetonitrile 90/10 + 0.05% trifluoroacetic acid (TFA); B, methanol +0.05% TFA): [minute/eluent B] 0'/40%; 2'/40%; 12'/100%; 22'/100%; 24'/40%; 30'/40%. Vesicles (50 μL), collected after FFE separation, were injected without any pretreatment. Sodium oleate and POPC were detected with a Corona charged aerosol detector (Thermo Scientific), and quantified by means of the respective calibration lines (Figure SI.3). Under these conditions, typical retention times were 11.6 min (sodium oleate), and 22.4 min (POPC), see Figure SI.4.

Cryo-Transmission Electron Microscopy. One droplet (6–10 μL) of the freshly prepared vesicle suspension was applied to a copper grid. Excess liquid was blotted for 3 s between two strips of filter paper. Subsequently, the samples (10–250 nm thick) were rapidly plunged into liquid ethane (−180 °C) in a Cryobox (Carl Zeiss NTS GmbH, Oberkochen, Germany). The samples were transferred using a cryo-transfer unit (Gatan 626-DH) into a precooled CM120 cryo-transmission electron microscope (Philips, Eindhoven, The Netherlands) operating at 120 kV and viewed under low-dose conditions. The images were recorded with a FastScan F1141kK CCD Camera (TVIPS, Gauting, Germany). Inner and outer vesicle diameters as well as the number of entrapped ferritin molecules were determined by means of image analysis using the ImageJ software (<http://rsb.info.nih.gov/ij/>). Intravesicular ferritin concentration was calculated accordingly.

Size Distribution and ζ -Potential Measurements. The vesicle size distribution was measured using a Zetasizer Nano ZS instrument (Malvern Instruments, Malvern, U.K.), at 25 °C. All samples were diluted to 1 mM (overall lipid concentration) for reducing turbidity. The instrument operates at a scattering angle of 173°. The refractive index and the viscosity of the 200 mM bicine buffer (sodium salt, pH 8.5) were approximated to the respective water values. Results are reported in terms of mean hydrodynamic diameter (Z-average diameter) and polydispersity index (PI), obtained by cumulative analysis of the correlation function. The same instrument was employed to measure the ζ potential (ζ , mV) of vesicles whose composition was varied from 100% oleate to 100% POPC. The correlation function was fitted by using standard instrumental parameters. The ζ potential of 100% POPC vesicles was also checked independently in a Malvern Zetasizer 5000, yielding consistent results.

Data Analysis. We will refer to the amount of sodium oleate micelles added to POPC vesicles by indicating the overall chemical composition of the oleate-POPC mixture. This is conveniently done by introducing the (overall) sodium oleate molar fraction x_{OL} , defined as

$$x_{OL} = \frac{[\text{oleate}]}{[\text{oleate}] + [\text{POPC}]}$$

where [oleate] and [POPC] represent the overall total sodium oleate plus oleic acid and POPC concentration, respectively. In addition to x_{OL} it is also useful to express the composition of oleate/POPC mixtures by using the oleate/POPC molar ratio r , that is defined as $r = [\text{oleate}]/[\text{POPC}]$. The two values are related by the equations:

$$x_{OL} = \frac{r}{1 + r}$$

$$r = \frac{x_{OL}}{1 - x_{OL}}$$

For example, when $x_{OL} = 0.2$, $r = 0.25$, this means that 1 equiv of oleate was added to 4 equiv of POPC, to give a total of 5 equiv of lipids (and [oleate]:[POPC] = 1:4). Typical values used in this work are summarized in Table SI.1.

In contrast to x_{OL} , which indicates the overall chemical composition of the vesicles plus micelles system (and is imposed by the experimental conditions), each vesicle subpopulation, as obtained after free-flow electrophoresis, has an actual oleate molar fraction that is indicated by y_{OL} . Note that y_{OL} is an experimentally determined value obtained by (1) comparing the position of vesicle peaks in the FFE electropherogram with "standard" peaks corresponding to vesicles of known composition, and (2) quantitative HPLC analysis of FFE-obtained vesicle fractions. In the case of high y_{OL} (>0.7), the agreement between these two different determinations becomes weaker, and a consensus value is obtained by averaging. This procedure was necessary due to the noise often associated with weak DPH fluorescence signals (high y_{OL}), and when FFE peaks overlap.

The fractional amount of lipids in each vesicle subpopulation is indicated by Q (%), defined as

$$Q = 100\% \times \frac{([oleate] + [POPC])_{subpopulation}}{([oleate] + [POPC])_{total}}$$

where the numerator refers to the lipid concentration in an FFE-obtained vesicle subpopulation (FFE peak), while the denominator refers to the total (overall) lipid concentration obtained by the addition of sodium oleate micelles to preformed POPC vesicles. Samples containing a single FFE peak have $Q_{peak} = 100\%$, while those containing two peaks have different Q values, with $Q_{peak1} + Q_{peak2} = 100\%$.

We noted that in vesicle subpopulations spreading among several FFE fractions, and in the case of partially overlapping FFE peaks, y_{OL} and Q values, which are related to each other by the simple algebraic equations (see Table SI.3), they do not fit perfectly with expectations. These divergences, however, do not affect the conclusions drawn in this paper.

3. RESULTS

First, we verified the assumption that pure oleate vesicles, pure POPC vesicles, and oleate/POPC mixed vesicles with various molar ratios have different electrokinetic potentials due to the different surface charge densities. In Figure 2, we report the variation of the ζ potential for oleate/POPC vesicles as a function of their composition. The ζ potential of pure POPC vesicles is slightly negative, about -2.5 mV, and it is likely a consequence of the solvent-induced dipole potential across the headgroup region of the bilayer. In contrast, the ζ potential of pure oleate vesicles in our working buffer (200 mM bicine, sodium salt, pH 8.5) is about -60 mV and the vesicles of intermediate composition show a monotonic profile with a steep initial variation when the oleate molar fraction is below 10%, and a more moderate trend in the remaining range.

This behavior can be rationalized by the classical Poisson–Boltzmann model for a dissociable surfactant that has a fixed pK value and is present in a planar membrane with mole fraction φ . The surface potential Φ_0 is then a solution of the algebraic equation

$$-\sinh\left(\frac{e\Phi_0}{2k_B T}\right) = \frac{2\varphi p_0}{1 + \exp\left(\frac{e\Phi_0}{k_B T}\right) 10^{pK - pH}} \quad (1)$$

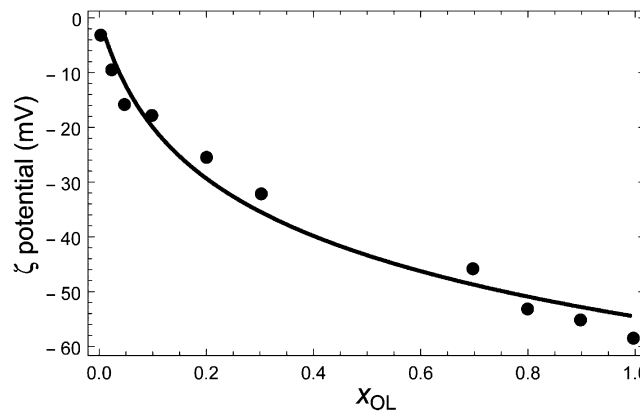


Figure 2. Biphasic variation of oleate/POPC vesicle ζ potential with the oleate content (overall lipid concentration: 1 mM). Filled circles represent the experimental data, whereas the solid line represent the variation of the surface potential Φ_0 with the oleate molar fraction, as calculated according to the Poisson–Boltzmann model, eq 1. Note that pure POPC vesicles have a slightly negative ζ potential in 200 mM bicine buffer, sodium salt (pH 8.5), as also reported in literature for similar cases. Presumably, it is due to membrane dipole potential.

where e denotes the elementary charge, k_B the Boltzmann constant, and T the absolute temperature, and $p_0 = 7$ is related to the buffer strength and the cross-sectional area of an oleate molecule in the membrane. The solid line in Figure 2 shows Φ_0 as predicted by eq 1 for $pK - pH = 0.035$.

Our experimental data together with the theoretical prediction suggest that the oleate amount in POPC vesicles correlates well with their ζ potential and therefore that vesicle behavior in an electric field can be explained in terms of oleate content.

Then we prepared oleate/POPC mixed vesicles with different compositions (x_{OL}) in order to verify that these populations can be separated by FFE. To detect lipid vesicles in the fractions obtained after the FFE separation, we employed diphenylhexatriene (DPH) as a lipid-soluble fluorescent probe. DPH fluorescence indicates the presence of membranes. DPH was added to each fraction, after the separation, according to a well-established method in our laboratory.¹⁹ This is a rapid procedure to identify the positions of the liposome peaks after the FFE separation but it might suffer from some quantitative limitations due to the dependence of DPH fluorescence on membrane composition. Preliminary studies suggest that the fluorescence signals of DPH in oleate and POPC vesicles differ considerably. In particular, POPC vesicles can be identified with a detection limit of ca. 10 μ M, while the values obtained can increase up to about 30 μ M in the case of oleate vesicles (Figure SI.5). At a given lipid concentration, DPH fluorescence is higher in POPC vesicles than in oleate vesicles, reflecting the different membrane compositions of the two (in terms of charge and fluidity). Mixed oleate/POPC vesicles display a DPH fluorescence that depends on their composition (data not shown).

Figure 3 shows typical electropherograms obtained when running oleate/POPC vesicles of different x_{OL} in the FFE device. The resulting 96 fractions were collected in a multiwell plate and the vesicles present in each fraction were detected fluorimetrically by adding DPH as described before. Depending on x_{OL} , vesicles move differently in the FFE apparatus and are thus collected in different wells. Typically, vesicles are spread over 5–10 adjacent wells but the FFE profile always consists of

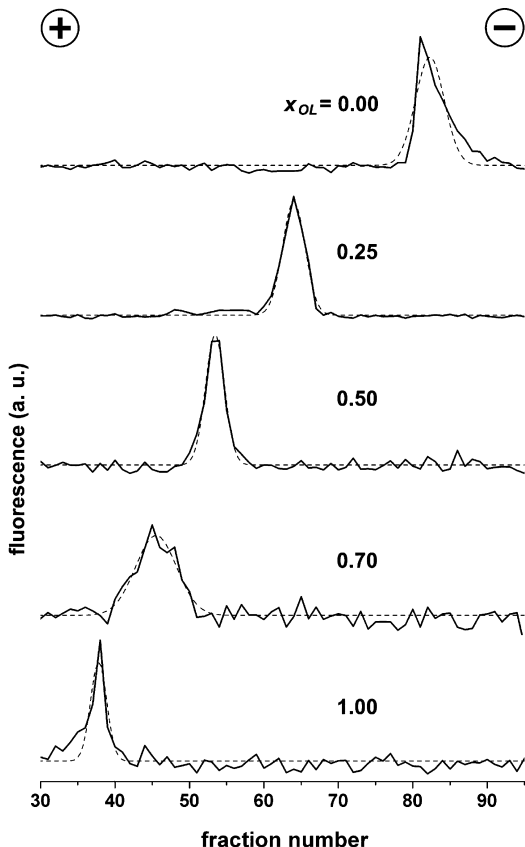


Figure 3. FFE calibration electropherograms of preformed oleate/POPC mixed vesicles, prepared at different oleate molar fractions x_{OL} (0, 0.25, 0.50, 0.70, 1.00, corresponding to oleate/POPC molar ratios r of 0, 1/3, 1, 7/3, ∞ , respectively). The lipid concentration of the samples varies with the oleate molar fraction (see Experimental Section for details), and it is always above 40 mM. The lipid concentration in the collected fractions is around one-tenth of the starting concentration. Lipid vesicles were made fluorescent by addition of DPH. Peaks were fitted with Gaussian functions and the maxima of each fitting function were taken as the central position of each peak. Fluorescence values (on the ordinate) are not to scale, in particular, when the oleate amount increases, DPH fluorescence decreases.

a single peak. POPC vesicles, which move along the apparatus almost unperturbed, are collected around fraction number 80. In contrast, negatively charged oleate vesicles are attracted by the anode and are typically collected in fractions 35–40. Vesicles of intermediate composition move accordingly. Note that the y -axis of Figure 3 represents the DPH fluorescence, which is not presented to scale. Actually, the fluorescence intensity decreases as the amount of oleate increases, (see Figure S1.5). These experiments demonstrate that oleate/POPC vesicles with different compositions can be separated by FFE.

The vesicle peaks in Figure 3 were fitted by a Gaussian function, so that the center of each peak can be evaluated despite the noisy electropherogram profile. The peak values were plotted against the chemical composition of the oleate/POPC vesicles injected into the apparatus, producing a calibration curve (Figure 4), which has been used to quantitatively determine the chemical composition of vesicles with unknown composition. This procedure allows us to determine the oleate molar fraction of each vesicle

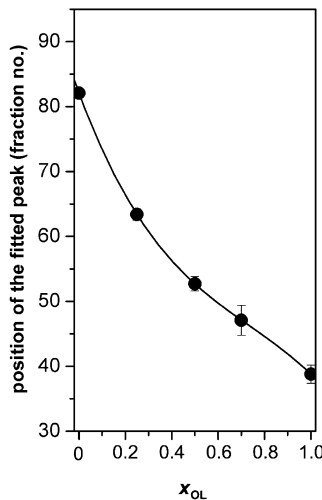


Figure 4. FFE calibration curve as obtained by injecting preformed oleate/POPC mixed vesicles in the FFE apparatus (Figure 3). The experimental data can be fitted by a polynomial function ($y = -43.8x^3 + 96.7x^2 - 96.4x + 82.1$), which was used to infer the composition y_{OL} of vesicle subpopulations by measuring the center of their FFE peaks ($n = 2$).

subpopulation (y_{OL}), which may differ from the overall molar fraction (x_{OL}).

In order to validate and refine the above-mentioned procedure based on the position of FFE peaks, we prepared and analyzed oleate/POPC vesicles with different oleate molar fractions (x_{OL}), and quantified the amounts of lipids in the FFE-fractions via HPLC. Note that x_{OL} represents the experimentally imposed oleate molar fraction, whereas y_{OL} represents the measured oleate molar fraction of each FFE peak. Very good agreement was found between the expected values and the values found in all electrophoretic peaks obtained in calibration experiments. For oleate/POPC preformed vesicles with x_{OL} from 0.2 to 0.7, the ratio between the observed and the expected amount of lipids is 1.00 ± 0.07 ($n = 40$ samples). For higher x_{OL} values, the ratio between the observed and the expected amounts of lipids decreases to about 0.6 ± 0.1 ($n = 13$ samples), indicating that in these cases a substantial amount of lipid is spread among multiple adjacent fractions, and that it is difficult to detect such vesicles as a clearly identifiable electrophoretic peak. For this reason, we combined HPLC data with the information obtained from the electropherogram to obtain a more reliable estimate of the composition and the amount of each population.

Finally, we carried out further experiments to check the behavior of oleate/POPC vesicles in the FFE apparatus; in particular we tested the effects of vesicle concentration and size. Vesicles of identical mean size and different concentrations (12.5–50 mM) are reproducibly recovered in the same collecting wells, and the DPH fluorescence signal changes as expected (Figures S1.6 and S1.7). Vesicles of identical concentration but different size (diameter: 100–200–400 nm) are also reproducibly collected in the same wells (Figure S1.8), so that we conclude that their separation in the FFE apparatus does not significantly depend on their size.

At this point, having shown that mixed oleate/POPC vesicles can be readily analyzed and separated by the FFE device, we proceeded with our investigation on the growth and transformation of oleate/POPC vesicles. This has been done by first using empty POPC vesicles (case study I), in order to

understand what happens to POPC vesicles upon addition of different amounts of oleate micelles. Subsequently, by using ferritin-filled POPC vesicles (case study II), we focused on the distribution of the entrapped solute molecules.

3.1. Case Study I. Addition of Oleate Micelles to Empty POPC Vesicles. We first used FFE separation to investigate the events upon feeding POPC vesicles with different amounts of oleate micelles. It is convenient to describe the experimental conditions by using the overall oleate molar fraction x_{OL} , which was varied between 0.2 and 0.91 (correspondingly, the oleate/POPC molar ratio r varied from 0.25 to 10). Figure 5 shows a collection of typical electropherograms. The experimental profiles, consisting of one or two electrophoretic peaks, were fitted with one or two Gaussian functions. When $x_{OL} \leq 0.29$ ($r \leq 0.4$), the vesicles resulting from the interaction between oleate micelles and preformed POPC vesicles are detected as a single peak, whereas for $x_{OL} \geq 0.4$ ($r \geq 0.67$), two peaks are observed. It is remarkable that FFE allows the detection of subpopulations of vesicles of different chemical composition, which are otherwise indistinguishable by other techniques. Using the FFE calibration curve (Figure 4) and HPLC analysis, we have calculated the oleate molar fraction (y_{OL}) and the fractional lipid amount Q (%) in each vesicle subpopulation. Whereas y_{OL} maintains the usual meaning (indicating the lipid composition of a certain vesicle subpopulation), Q indicates the fractional amount of lipids (POPC + oleate) in each subpopulation (for example, in the case of two subpopulations, one could contain 20% of the lipids, and the other the remaining 80%).

Results are shown in Table 1 and are graphically reported in Figures 5, 6, and SI.9.

It appears from Figure 5 and Table 1 that the system behaves differently for low and high x_{OL} values. Let us discuss these cases separately.

When a small amount of oleate is added, specifically for $x_{OL} \leq 0.29$ ($r \leq 0.4$), only one vesicle population is formed, as evidenced by the electropherogram. For this condition (entries 1–3 of Table 1), the chemical composition of the formed vesicles largely agrees with the predicted values (as revealed by their position in the electropherogram, their peak area, and as further confirmed by HPLC analysis). By increasing the amount of added oleate micelles, the resulting oleate/POPC vesicle peaks move to the left in the electropherograms, as expected (compare with Figure 3). The behavior of the system in this regime can be explained in the following manner: preformed POPC vesicles take up all the added oleate micelles, thus forming one single population of vesicles. This population is homogeneous in terms of its chemical composition y_{OL} , which in turn corresponds to a single overall oleate molar fraction x_{OL} .

When a larger amount of oleate micelles is added, specifically for $x_{OL} \geq 0.4$ ($r \geq 0.67$), the system behaves differently (entries 4–7, Table 1). Under these conditions, two peaks appear in the electropherograms, indicating the presence of two physically distinct vesicle populations. Specifically, the centers of the two bands move together toward the anode (to the left-hand side of the electropherogram), and whereas the area under one peak decreases, the area under the other peak increases as the amount of oleate micelles increases.

Results reported in Table 1 and Figure 6 suggest that above a certain threshold x_{OL} oleate micelles are not simply incorporated into the preformed POPC vesicles, as occurs in the first regime. Instead, two vesicle populations emerge via a

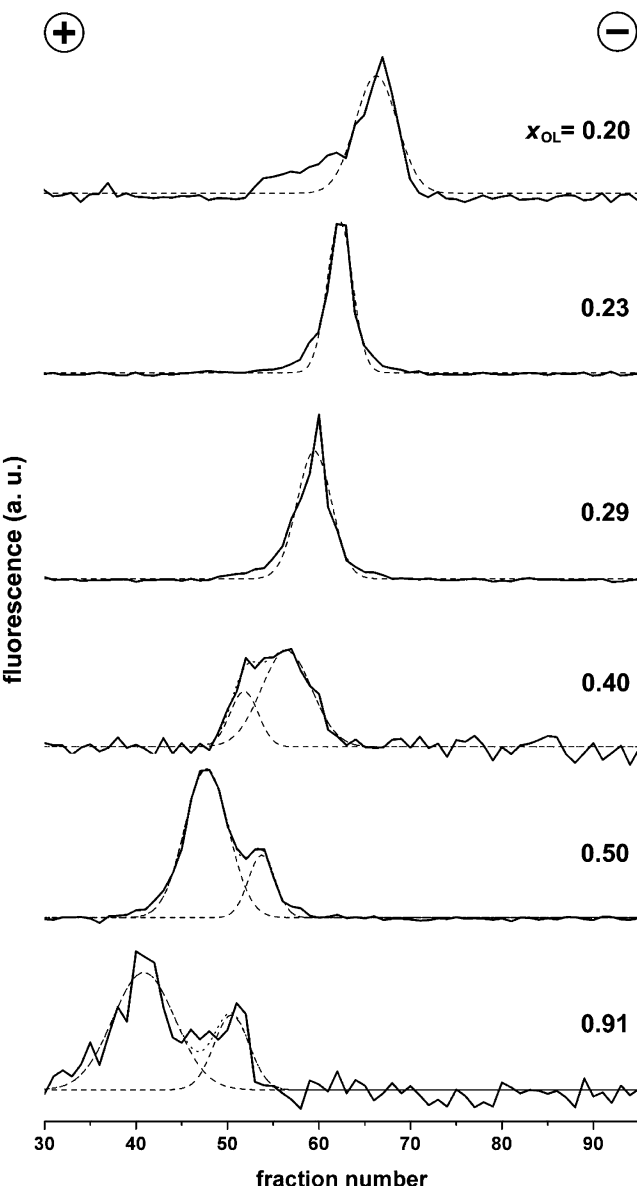


Figure 5. FFE analysis of vesicles obtained by adding different amounts of oleate micelles to preformed POPC vesicles. Oleate micelles were added in order to obtain an overall composition x_{OL} (shown values corresponding to oleate/POPC molar ratios r of 1/4, 3/10, 4/10, 2/3, 1, and 10, respectively). Lipid vesicles were made fluorescent by addition of DPH. FFE peaks were fitted with one or two Gaussian functions, and the peak positions obtained after fitting were taken as the center of vesicle subpopulation peaks. When $x_{OL} = 0.4$, 0.5, and 0.91 the two resulting vesicle populations were designated “oleate-rich” (left peak, high y_{OL}) and “oleate-poor” (right peak, low y_{OL}). Fluorescence values (on the ordinate) are not to scale; in particular, when the oleate amount increases, DPH fluorescence decreases.

more complex process. The chemical composition of the two vesicle populations follows a trend, according to the variation of the overall oleate molar fraction x_{OL} . The oleate molar fraction of “oleate-poor” vesicles ($y_{OL,\text{poor}}$) goes up from 0.41 to 0.45, then further to 0.76, whereas in the case of “oleate-rich” vesicles ($y_{OL,\text{rich}}$), it increases from 0.54 to 0.60, then to 0.94. The amount of lipids in each population (expressed as percent abundance Q) varies accordingly (see Table 1 and Figure SI.9). In particular, the amount of oleate-poor vesicles decreases from

Table 1. Chemical Composition and Lipid Amount of Vesicle Populations Obtained after FFE Separation

no.	overall oleate molar fraction x_{OL}	oleate/POPC molar ratio (r)	FFE peaks	center of the peak (fraction number)	found y_{OL} (FFE)	consensus y_{OL} (FFE and HPLC)	consensus Q (FFE and HPLC) [%]
Without Ferritin							
1	0.20	0.25	1	65.0	0.22	0.20 ± 0.03	100
2	0.23	0.3	1	62.4	0.27	0.26 ± 0.02	100
3	0.29	0.4	1	59.5	0.34	0.34 ± 0.01	100
4	0.40	0.67	2	51.8	0.54	0.54	27
				57.0	0.39	0.39	73
5	0.50	1	2	48.1	0.66	0.60 ± 0.08	52 ± 16
				54.5	0.46	0.45 ± 0.01	48 ± 16
6	0.91	10	2	40.9	0.92	0.94 ± 0.03	89 ± 7
				50.4	0.58	0.76 ± 0.25	11 ± 7
With Ferritin							
7	0.5	1	2	49.5	0.61	0.61	—
				54.6	0.46	0.46	—
8	0.67	2	2	45.3	0.75	0.75	67 ± 15
				51.3	0.56	0.56	34 ± 15

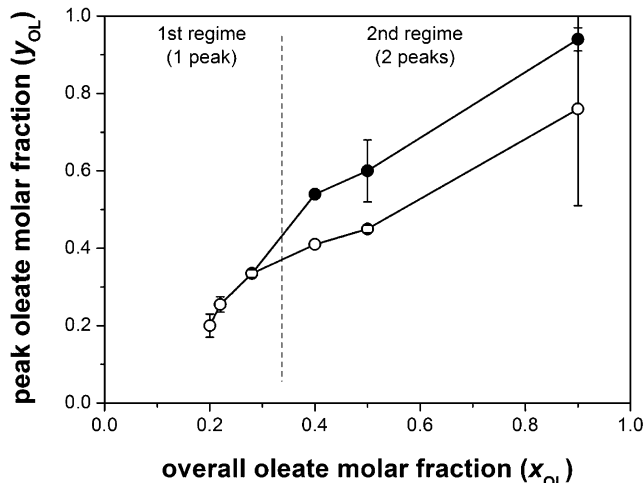


Figure 6. Variation of the oleate molar fraction (y_{OL}) in the vesicle subpopulations at different experimental conditions as determined by the overall composition (here indicated by the overall oleate molar fraction x_{OL}). Two regimes are clearly evident; cf. Figures 5 and S9. When $x_{OL} < 0.35$, only one vesicle population emerges, whose chemical composition (y_{OL}) is equal, within the experimental error, to x_{OL} . When $x_{OL} > 0.35$, two subpopulations emerge, here indicated by open circles (oleate-poor, low y_{OL}) and filled circles (oleate-rich, high y_{OL}). The large error bars associated with the last sample ($x_{OL} = 0.91$) are due to difficulties in accurately determining the center of peaks in the electropherograms.

73 to 11%, whereas the amount of oleate-rich vesicles increases accordingly. Even if these figures should be taken with some caution (see [experimental](#) part), the data clearly show a trend revealing the spontaneous onset of two chemically and physically distinct populations, as the amount of added oleate micelles increases.

To summarize, the addition of oleate micelles to POPC vesicles yields two different reaction patterns depending on the amount of added oleate. We can define a threshold value of $x_{OL}^* \approx 0.35$ to characterize the transition from the first to the second regime. We shall see that these two regimes might be interpreted as corresponding to two different processes (i.e., growth or growth-division).

3.2. Case Study II. Addition of Oleate Micelles to Ferritin-Filled POPC Vesicles.

In order to obtain more

insights into the mechanism of oleate micelle uptake by preformed POPC vesicles, we investigated the events occurring when solutes are present inside the vesicles during their growth and division. To this end, we needed a suitable marker for the vesicle lumen. Ferritin is a large protein (diameter ca. 12.5 nm) composed of 24 subunits, assembled as a shell around a core composed of ferric oxide phosphate. Ferritin molecules are clearly visible as black spots in electron microscopy images.

Ferritin-containing POPC vesicles were produced by reverse phase evaporation and then extruded through 100 nm pores. After removal of free ferritin by size exclusion chromatography, oleate micelles were added, to the extent that $x_{OL} = 0.5$ or 0.67 ($r = 1$ or 2). The mixture was then applied to the FFE apparatus for vesicle fractionation. As expected, in both cases two vesicle populations emerged, quite consistently with the results shown for “empty” vesicles in Figures 5 and 6. Detailed data are reported in Table 1 (entries 7–8). The positions and the areas of the peaks fit well with those determined for vesicles without ferritin. This means that the presence of internalized solutes does neither significantly affect the oleate uptake nor the subsequent transformation of the resulting oleate/POPC vesicles.

The initial ferritin-filled POPC vesicles, as well as the vesicles produced upon oleate micelle addition (collected from the FFE apparatus) were then analyzed by cryo-TEM, in order to visualize their ferritin content (Figure 7).

Figure SI.10ab shows typical micrographs that reveal the presence of ferritin-containing POPC vesicles before the addition of oleate micelles. Note that nonentrapped ferritin was removed by size exclusion chromatography. We estimated the average intravesicular ferritin concentration by direct counting of the number of ferritin molecules inside 78 ferritin-filled unilamellar POPC vesicles (empty vesicles were excluded), obtaining an average value of $25 \mu\text{M}$. This value is lower than the concentration of ferritin prevailing during the formation of the vesicles by the reverse phase evaporation method ($60 \mu\text{M}$), indicating that the larger proportion of the ferritin molecules had been lost, not unexpectedly, during the last step of the reverse-phase evaporation procedure (in particular, during the final gel-to-vesicle rearrangement).

In the next step, we analyzed the morphology of vesicles from the two populations obtained after FFE separation. A typical micrograph of oleate-poor vesicles is presented as Figure

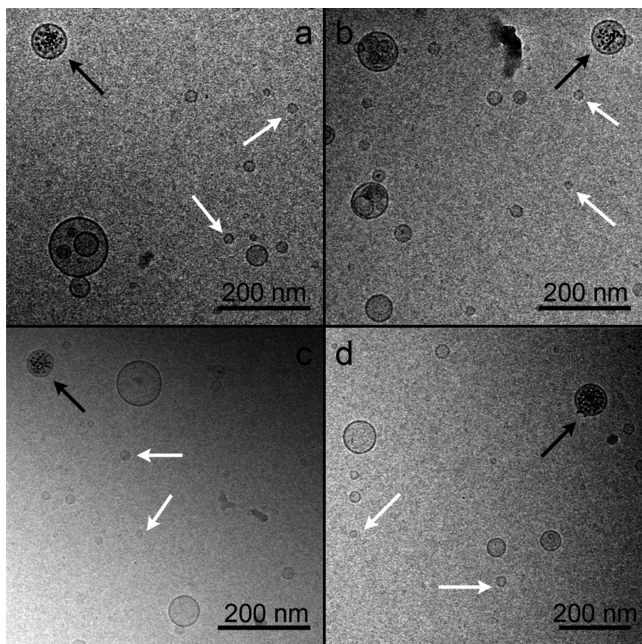


Figure 7. Cryo-TEM images of oleate-rich vesicles (y_{OL} ca. 0.6) as obtained after oleate micelle addition to ferritin-containing POPC vesicles, under 1:1 condition ($x_{OL} = 0.5$). Note the simultaneous presence of large filled vesicles (black arrows), large empty vesicles, and small empty vesicles (white arrows). The presence of the latter could also be due to imperfect separation (cf. Figure SI.10c).

SI.10c, and refers to the outcome of both experiments (Table 1, entries 7 and 8). These are quite small vesicles (diameter around 30–40 nm) and rarely contain ferritin molecules. On the other hand, oleate-rich vesicles are both small and large; moreover, ferritin is present inside vesicles belonging to this oleate-rich subpopulation, and generally in vesicles with larger size.

By comparing the vesicle size distribution of the ferritin-filled vesicles before and after oleate micelle addition (i.e., the preformed POPC vesicles versus the oleate-rich vesicle population) it appears that both size (diameter) and the intravesicular ferritin concentration distributions of the two samples are statistically significantly different ($p < 0.05$; see Figures SI.11 and SI.12 for statistical details). In particular, the average size decreases from 122 to 103 nm; whereas the average intravesicular ferritin concentration increases from 25 to 61 μM . As discussed below, the increase of ferritin concentration cannot be explained only by the modest reduction of vesicle size (−16%).

Quite remarkably, in addition to the mean increase of intravesicular ferritin concentration, we were able to identify “special” vesicles (see Figure 8) whose internal ferritin concentration was much higher than the average (61 μM), even up to 200 μM , i.e., about 1 order of magnitude higher than the average ferritin concentration inside preformed POPC vesicles (25 μM). The existence of such vesicles within the oleate-rich population suggests that under particular conditions, the mechanism that leads to an increase of ferritin concentration (from 25 to 61 μM) can be amplified to reach a ca. 10-fold increase.

In contrast to the oleate-rich vesicle population, composed of large vesicles that are very often filled with ferritin, the oleate-poor population is represented by quite small empty vesicles. Their average size lies around 40 nm. It should be emphasized

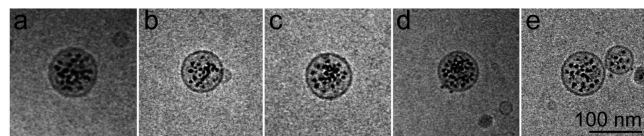


Figure 8. Special ferritin-containing vesicles found in the sample after the growth-division process. The concentration of ferritin inside these vesicles (160–200 μM) is much higher than the average intravesicle ferritin concentration of the mother vesicles from which they were generated (~25 μM). The local ferritin concentration is calculated by direct counting the number of entrapped ferritin molecules and by measuring vesicle size. Note that ferritin molecules are not aggregated. Images refer to samples whose composition is specified in Table 1 (entries #7 and #8), in particular, from left to right, $x_{OL} = 0.5, 0.5, 0.67, 0.67$, and 0.67.

that these are not *de novo* formed oleate vesicles (produced by the spontaneous micelle-to-vesicle transition, as reported^{5,6}), since their lipid composition is POPC-rich. Rather, these small vesicles represent the product of a rearrangement mechanism that involves the preformed POPC vesicles. The absence of entrapped ferritin, however, suggests a very peculiar generative mechanism.

When we consider together the oleate-rich and oleate-poor fractions, the overall size distribution is shifted to lower sizes, as compared to the initial one. In agreement with the data reported previously,^{7,11,12} this suggests a mechanism of fission of the initial vesicles, which we have hypothesized initially,^{2,5,6} but which was difficult to detect by a dynamic light scattering (DLS) analysis. In fact, as shown in Figure SI.13, the intensity-weighted mean diameter (Z-average) derived from DLS data using the cumulative analysis, does not change significantly. The polydispersity index, however, does change, revealing—although less conspicuously—that at high oleate-to-POPC ratios, some changes in the vesicle size distribution do indeed occur.

4. DISCUSSION

Previous work on the addition of oleate micelles to preformed POPC vesicles was carried out typically at $x_{OL} \geq 0.5$ ($r \geq 1$). On the basis of spectroscopic,^{7,11,12} and microscopic,^{5,6} investigations (and partially on chromatographic studies as well^{20–22}) we proposed that the main occurring process is the growth and division of POPC vesicles owing to the uptake of oleate micelles, possibly in parallel with the formation of some new vesicles from a direct oleate micelles-to-vesicles transformation route (*de novo* vesicle formation). The term “vesicles self-reproduction” describes the net result: the formation of new vesicles starting from pre-existing vesicles. As emphasized in the introduction, this mechanism bears relevance to origin-of-life scenarios because it provides a spontaneous route to proliferation of primitive cells without the need of sophisticated biochemical machineries. A detailed comment on previous knowledge can be found in the Supporting Information.

This study corroborates the self-reproduction mechanism, but two new important points emerge, that need discussion and future investigations: (i) the existence of a threshold oleate molar fraction ($x_{OL}^* \approx 0.35$) that distinguishes two regimes when oleate micelles are added to preformed POPC vesicles ($x_{OL} < 0.35$, growth; $x_{OL} > 0.35$, growth–division); (ii) the redistribution of entrapped ferritin molecules (as observed when $x_{OL} = 0.5$ and 0.67).

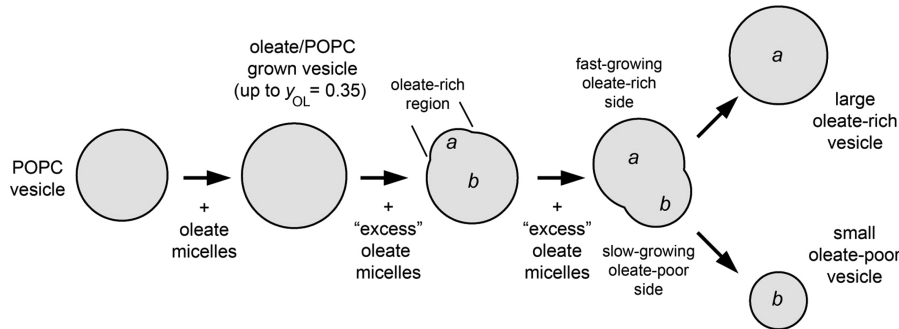


Figure 9. Hypothetical and simplified mechanism of POPC vesicle growth and division after the uptake of oleate micelles. The preformed POPC vesicles, possibly containing ferritin, first take up a limited amount of micelles and grow to yield a mixed oleate/POPC vesicle with $y_{OL} \sim 0.35$. This is the behavior observed when $x_{OL} \leq \text{ca. } 0.35$. Consequently, only one vesicle population is observed in FFE analysis. By contrast, when more oleate micelles are added (so that $x_{OL} > 0.35$), the “excess” oleate molecules are taken up by the grown vesicles, stochastically forming small oleate-rich regions in the membrane. We claim that the dissymmetric growth rate of oleate-rich (fast growing) and oleate-poor regions (slow growing) is the main cause of vesicle deformation and division, and explains in a quantitative manner both the composition (y_{OL}) and the relative amount (Q) of the resulting daughter vesicles (on the rightmost side of the figure). In first approximation, internal solutes (not shown) will be partitioned among the daughter vesicles according to their relative volumes, but quantitative estimations can only partially account for the experimental observations—based on the protein ferritin. In particular, the redistribution of ferritin is much more “polarized” than expected (oleate-rich vesicles contain more solute molecules than the calculated value; oleate-poor vesicles are much smaller than expected and rarely contain ferritin molecules). Note that additional processes can take place (e.g., oleate uptake from the vesicles formed after division) and that a vast combination of microscopic possibility cannot be discriminated by available data; see text for more details.

When a small amount of oleate micelles is added to POPC vesicles ($x_{OL} < 0.35$), only one chemically homogeneous vesicle population is formed, and—as expected—the oleate molar fraction of the vesicles y_{OL} is equal to the overall oleate molar fraction x_{OL} . This suggests that all POPC vesicles quickly take up oleate molecules from the added micelles, resulting in simple vesicle growth. Strong membrane perturbations of POPC vesicles within this x_{OL} range appear to be unlikely because when $x_{OL} < 0.35$ the expected surface increase of a POPC vesicle that takes up all available oleate molecules is less than 24% (radius increase <11%). This is due to the smaller oleate headgroup area (0.32 nm^2), when compared to POPC (0.72 nm^2).¹²

On the other hand, when more oleate micelles are added to POPC vesicles ($x_{OL} > 0.35$), two vesicle populations appear in the FFE profile, conveniently referred to as “oleate-rich” and “oleate-poor” vesicles. Their chemical compositions ($y_{OL,\text{rich}}$ and $y_{OL,\text{poor}}$) differ from the overall lipid composition (x_{OL}), being—respectively—higher and lower than x_{OL} . The oleate-rich vesicles represent the minor component when $x_{OL} = 0.4$, appear approximately in the same amounts as the oleate-poor vesicles when $x_{OL} = 0.5$, and become dominant for higher x_{OL} values (Table 1 and Figure SI.9). In this case the insertion of oleate molecules brings about a strong perturbation of the POPC membrane that changes vesicle stability and causes a rearrangement (growth-division).

According to recent findings (based, however, on DOPC/oleate rather than on POPC/oleate) it cannot be excluded that the addition of oleate molecules on POPC membrane might induce a local phase transition as soon as a certain local molar fraction is reached.²³ In particular it has been shown that a transition from lamellar to cubic phase occurs, likely producing a chemical demixing of membrane constituents.

It is remarkable that two populations with different lipid compositions emerge from the oleate micelle/POPC vesicle interaction, and since our measurements were performed several minutes after oleate/micelle mixing, this out-of-equilibrium distribution is rather persistent and implies differences in the rates of oleate uptake (k_{on}), release (k_{off}) in

membranes with different phospholipid content and possibly different size (specific work on this issue was recently published^{24,25}). Note that the preliminary validation experiments, described in section 3, serve to rule out the possibility that the appearance of multiple peaks during the analysis of oleate/POPC mixed vesicles were FFE-induced artifacts, possibly caused by intervesicle oleate transfer within the FFE apparatus.

In order to explain the observations, we first asked whether any characteristic physical constraint occurs near the “critical point”, specifically when x_{OL} is about 0.35. Note that this corresponds approximately to the addition of 0.5 equiv of oleate to one equivalent of POPC.

This critical value is clearly not related to “chemical” saturation of POPC membranes from oleate (because oleate/POPC vesicles can be prepared in any molar ratio), but should derive from the mechanism of oleate uptake, possibly involving local changes of the membrane curvature or formation of nonlamellar regions, because of oleate accumulation.

Numerical analysis reveals that the geometrical saturation of POPC vesicles surface by a layer of closely packed oleate micelles¹⁴ is not relevant in the present case (see Table SI.1).

We noted instead that the composition (y_{OL}) and the relative lipid amount (Q) of the vesicle subpopulations obtained when $x_{OL} > 0.35$ can be explained quite adequately by considering that a certain amount of added oleate is first incorporated into POPC vesicles, bringing about pure growth (i.e., up to $y_{OL} = 0.35$), whereas the subsequent incorporation of the remaining oleate (the “excess” oleate), makes the grown vesicles unstable, so that they divide and yield oleate-rich and oleate-poor daughter vesicles.

Table SI.2 shows that the calculated y_{OL} and Q values for oleate-poor and oleate-rich vesicles fit quite well with the experimentally determined values under the hypothesis that 80% of the excess oleate ends up in oleate-rich vesicles, and the remaining 20% in oleate-poor vesicles. This would imply that the grown vesicles ($y_{OL} = 0.35$) diverge from symmetric growth by further uptake of oleate.

Necessarily, this mechanism must be based on effects that depend on local membrane composition. An intriguing possibility is the cooperative formation of oleate-rich regions in the membrane of growing POPC vesicles. The oleate-rich regions could be stabilized against repulsion by a hydrogen bond network, in accord with current knowledge on fatty acid/soap membranes,²⁶ and their existence has been suggested long time ago after electrophoretic mobility studies.²⁷ As tentatively justified in the Supporting Information, the oleate-rich regions, owing to their different local properties would preferentially take up oleate molecules and grow faster than oleate-poor regions, possibly with local increment of flip-flop rates. The divergence from a spherical geometry, in turn, would favor vesicle division.^{8,28}

Fast-growing oleate-rich regions would lead—after division—to oleate-rich vesicles of large size, and slow-growing oleate-poor regions to small oleate-poor vesicles. To fit the data, we have made the hypothesis that the fast-growing regions (oleate-rich) grow about four times faster than the slow-growing regions (oleate-poor) (Table SI.2). However, comparison between these estimates and the actual diameters of vesicles after division suggests that whereas oleate-rich vesicles should derive from a simple grow–division mechanism, oleate-poor ones (being too small) derive from a further rearrangement/fragmentation step.

It is important to remark that this is a simplified explanation and it does not take into account the certainly complex and multiple pathways that actually could involve not only the preformed POPC vesicles, but also the *in situ* generated POPC/oleate mixed daughter vesicles. A cascade mechanism would generate a vast combination of possibilities, whose occurrence, however, is difficult to detect by just observing the final state (as done in this work). In other words, the proposed model (Figure 9) could be complemented by additional processes.

A hint that this is indeed the case comes from several facts, namely: (i) vesicles of different sizes are always obtained, also in “pure” electrophoretic fractions, indicating that a multitude of pathways exists; (ii) an equal number of oleate-rich and oleate-poor vesicles should be obtained by an ideal division process, but instead we measured an equal lipid amount among the two populations (Figure SI.9) suggesting that the number of small oleate-poor vesicles is higher than the number of large oleate-rich ones; finally, (iii) evidence based on vesicle diameters and ferritin content also imply more complex pathways (see also Section 3.2).

An intriguing question is whether the mechanism of asymmetric vesicle growth and division as discussed above is consistent with the second set of observations, i.e. the concentration and the redistribution of ferritin inside vesicles.

Experiments with ferritin-containing vesicles, carried out with $x_{OL} = 0.5$ and 0.67 , show that the ferritin molecules contained in the preformed POPC vesicles (average diameter: 123 nm; average concentration: $25 \mu\text{M}$) are generally found inside oleate-rich vesicles (103 nm, $61 \mu\text{M}$), whereas the vast majority of oleate-poor vesicles, which are significantly smaller (40 nm), are generally empty (Figures 7, 8, and SI.10).

Since the number of entrapped ferritin molecules is proportional to vesicle volume, it is not surprising that the small oleate-poor vesicles are generally empty even if they derive from ferritin-filled mother vesicles. Their captured volume is small when compared with the oleate-rich large vesicles and moreover these small vesicles could actually derive

from sequential rearrangement/fragmentation steps (note that during each division step entrapped solutes can be lost to the environment).

When ferritin-filled oleate-rich vesicles are considered, instead, the interesting conclusion is that the internal ferritin concentration is higher than expected. In fact, even if all ferritin molecules initially present in the mother vesicles were transferred preferentially only to the oleate-rich daughter vesicles (and no one is lost during division), an average intravesicular ferritin concentration of $44 \mu\text{M}$ is expected, whereas a value as high as $61 \mu\text{M}$ is actually measured. Moreover, we also observed a small number of exceptionally filled vesicles (Figure 8). This concentration difference ($61 \mu\text{M} - 44 \mu\text{M} = +17 \mu\text{M}$) is statistically significant within the samples (79 and 140 vesicles, before and after growth–division, respectively), but future and more detailed investigations will allow more accurate analysis of this phenomenon.

When trying to unravel the underlying mechanism of this intriguing solute concentration in daughter vesicles the discussion becomes inevitably more speculative. These ferritin-stuffed vesicles necessarily derive from a sort of condensing mechanism based on solute–solute and solute–membrane interactions. In earlier work on ferritin and ribosome entrapment,^{29,30} it was proposed that macromolecular solutes could play a kinetic role during closed vesicle formation from open bilayer discs.

Here a similar mechanism could operate, whereby the starting point is not an open bilayer disc, but rather the self-sealing membrane at the moment of vesicle division. A mechanism reminiscent of the hydrophobic effect, causing water molecules to be liberated by exclusion phenomena could also be the driving force in this case.

Kinetic and thermodynamic factors, taken all together, would favor those pathways that bring about the formation of solute-filled vesicles. Possibly, the very special superfilled vesicles pictured in Figure 8 (up to $200 \mu\text{M}$), derive from those cases where local microconditions favor this phenomenon.

CONCLUDING REMARKS

In this study, we have shown that vesicles obtained after addition of oleate micelles to preformed POPC vesicles are heterogeneous in terms of lipid composition, as evidenced by an FFE fractionation procedure. On the basis of previous evidence on vesicle growth–division (i.e., self-reproduction),^{2,3,5–7} we tentatively explain this observation by considering that local cooperative effects can favor the uptake of oleate molecule with different rates in different regions of the POPC vesicle membrane. This in turn brings about an asymmetric growth that leads, after division, to oleate-rich and oleate-poor vesicles.

Following vesicle division, some new vesicles will contain most of the solutes (ferritin) initially entrapped in the mother vesicles, while others will not contain any solute. While most of the ferritin-filled vesicles contain a somewhat larger amount of ferritin molecules than the expected value ($61 \text{ vs } 44 \mu\text{M}$), only very few are expected to contain extraordinarily high solute concentrations (up to $200 \mu\text{M}$). We propose that this is the reflection of a spontaneous self-concentration pathway—induced by vesicle growth–division—that might enrich the fraction of solutes-rich vesicles. We have used ferritin as a model protein, but also other macromolecules (enzymes, RNA) might display this behavior. As the spontaneous formation of solutes-rich vesicles models the formation of solute-filled

primitive cells, our results might be relevant in an origin-of-life scenario, where the issue of solute concentration inside compartments is crucial.^{29–31} Solute-rich primitive cells could effectively compete with the solute-poor ones and being selected for the onset of primitive metabolism.

Although this work provides some new insights with respect to the previous state-of-art, it also poses new unsolved questions. What would happen in the case of recursive addition of fresh oleate micelles or new POPC vesicles? Previous knowledge indicates that the “matrix effect” still operates when a large excess of oleate micelles is added to POPC preformed vesicles.¹² Mixed vesicles are quickly formed when x_{OL} increases up to 0.99 and unpublished observations suggest that the effect is only partially lost when x_{OL} reaches 0.999, meaning that even small amounts of POPC molecules can modify the oleate vesicle formation. Additional evidence of alteration of fatty acid vesicle growth rates by small amounts of phospholipids have been recently reported.²⁴ Similarly, previous work has shown that if POPC vesicles are added to preformed oleate vesicles, a dynamical pattern takes place again, oleate molecules are taken up by POPC vesicles, which grow and divide.³² Such evidence were originally obtained by dynamic light scattering and spectroturbidimetry, but given the charged nature of the vesicles used, FFE analysis could help for further mechanistic investigations. Moreover, detailed theoretical models,^{25,33} especially stochastic ones, can further support future mechanistic investigations.

■ ASSOCIATED CONTENT

S Supporting Information

The Supporting Information is available free of charge via the Internet at <http://pubs.acs.org/>. The Supporting Information is available free of charge on the ACS Publications website at DOI: [10.1021/acs.jpcb.5b05057](https://doi.org/10.1021/acs.jpcb.5b05057).

Supporting text (sections SI.1–SI.4); Figures SI.1–SI.13; Tables SI.1–SI.3 ([PDF](#))

■ AUTHOR INFORMATION

Corresponding Authors

*(A.F.) E-mail: Alfred.Fahr@uni-jena.de.

*(P.L.L.) E-mail: luisi@mat.ethz.ch.

Present Address

[#](T.P.S.) Department of Earth and Planetary Sciences, Harvard University, Cambridge, MA 02142

Notes

The authors declare no competing financial interest.

■ ACKNOWLEDGMENTS

This work derived from our recent involvement (A.F. and P.L.L.) in studies on the construction of semisynthetic minimal cells, funded by the FP6-EU Program (*SynthCells* project, No. 43359). We thank Mukul Ashtikar (Institut für Pharmazie, Friedrich Schiller Universität Jena) for helping with Corona CAD HPLC analyses. T.P.d.S. was supported by the Alexander von Humboldt Foundation as a postdoctoral fellow in Jena, Germany.

■ REFERENCES

- Bachmann, P. A.; Luisi, P. L.; Lang, J. Autocatalytic Self-Reproducing Micelles as Models for Prebiotic Structures. *Nature* **1992**, *357*, 57–59.

(2) Walde, P.; Wick, R.; Fresta, M.; Mangone, A.; Luisi, P. L. Autopoietic Self-Reproduction of Fatty Acid Vesicles. *J. Am. Chem. Soc.* **1994**, *116*, 11649–11654.

(3) Stano, P.; Luisi, P. L. Achievements and Open Questions in the Self-Reproduction of Vesicles and Synthetic Minimal Cells. *Chem. Commun.* **2010**, *46*, 3639–3653.

(4) Szostak, J. W.; Bartel, D. P.; Luisi, P. L. Synthesizing Life. *Nature* **2001**, *409*, 387–390.

(5) Berclaz, N.; Müller, M.; Walde, P.; Luisi, P. L. Growth and Transformation of Vesicles Studied by Ferritin Labeling and Cryotransmission Electron Microscopy. *J. Phys. Chem. B* **2001**, *105*, 1056–1064.

(6) Berclaz, N.; Blöchliger, E.; Müller, M.; Luisi, P. L. Matrix Effect of Vesicle Formation as Investigated by Cryotransmission Electron Microscopy. *J. Phys. Chem. B* **2001**, *105*, 1065–1071.

(7) Rasi, S.; Mavelli, F.; Luisi, P. L. Cooperative Micelle Binding and Matrix Effect in Oleate Vesicle Formation. *J. Phys. Chem. B* **2003**, *107*, 14068–14076.

(8) Zhu, T. F.; Szostak, J. W. Coupled Growth and Division of Model Protocell Membranes. *J. Am. Chem. Soc.* **2009**, *131*, 5705–5713.

(9) Mansy, S. S.; Szostak, J. W. Reconstructing the Emergence of Cellular Life through the Synthesis of Model Protocells. *Cold Spring Harbor Symp. Quant. Biol.* **2009**, *74*, 47–54.

(10) Kurihara, K.; Tamura, M.; Shohda, K.; Toyota, T.; Suzuki, K.; Sugawara, T. Self-Reproduction of Supramolecular Giant Vesicles Combined with the Amplification of Encapsulated DNA. *Nat. Chem.* **2011**, *3*, 775–781.

(11) Blochlinger, E.; Blocher, M.; Walde, P.; Luisi, P. L. Matrix Effect in the Size Distribution of Fatty Acid Vesicles. *J. Phys. Chem. B* **1998**, *102*, 10383–10390.

(12) Lonchin, S.; Luisi, P. L.; Walde, P.; Robinson, B. H. A Matrix Effect in Mixed Phospholipid/Fatty Acid Vesicle Formation. *J. Phys. Chem. B* **1999**, *103*, 10910–10916.

(13) Stano, P.; Wehrli, E.; Luisi, P. L. Insights into the Self-Reproduction of Oleate Vesicles. *J. Phys.: Condens. Matter* **2006**, *18*, S2231–S2238.

(14) Chen, I. A.; Szostak, J. W. A Kinetic Study of the Growth of Fatty Acid Vesicles. *Biophys. J.* **2004**, *87*, 988–998.

(15) Peterlin, P.; Arrigler, V.; Kogej, K.; Svetina, S.; Walde, P. Growth and Shape Transformations of Giant Phospholipid Vesicles upon Interaction with an Aqueous Oleic Acid Suspension. *Chem. Phys. Lipids* **2009**, *159*, 67–76.

(16) De Cuyper, M.; Joniau, M.; Dangreau, H. Spontaneous Phospholipid Transfer between Artificial Vesicles Followed by Free-Flow Electrophoresis. *Biochem. Biophys. Res. Commun.* **1980**, *95*, 1224–1230.

(17) De Cuyper, M.; Joniau, M.; Dangreau, H. Intervesicular Phospholipid Transfer. A Free-Flow Electrophoresis Study. *Biochemistry* **1983**, *22*, 415–420.

(18) Szoka, F., Jr.; Papahadjopoulos, D. Procedure for Preparation of Liposomes with Large Internal Aqueous Space and High Capture by Reverse-Phase Evaporation. *Proc. Natl. Acad. Sci. U. S. A.* **1978**, *75*, 4194–4198.

(19) Holzer, M.; Momm, J.; Schubert, R. Lipid Transfer Mediated by a Recombinant Pro-sterol Carrier Protein 2 for the Accurate Preparation of Asymmetrical Membrane Vesicles Requires a Narrow Vesicle Size Distribution: A Free-Flow Electrophoresis Study. *Langmuir* **2010**, *26*, 4142–4151.

(20) Chungcharoenwattana, S.; Ueno, M. Size Control of Mixed Egg Yolk Phosphatidylcholine (EggPC)/Oleate Vesicles. *Chem. Pharm. Bull.* **2004**, *52*, 1058–1062.

(21) Chungcharoenwattana, S.; Ueno, M. New Vesicle Formation upon Oleate Addition to Preformed Vesicles. *Chem. Pharm. Bull.* **2005**, *53*, 260–262.

(22) Chungcharoenwattana, S.; Kashiwagi, H.; Ueno, M. Effect of Preformed Egg Phosphatidylcholine Vesicles on Spontaneous Vesiculation of Oleate Micelles. *Colloid Polym. Sci.* **2005**, *283*, 1180–1189.

- (23) Gillams, R. J.; Nylander, T.; Plivelic, T. S.; Dymond, M. K.; Attard, G. S. Formation of Inverse Topology Lyotropic Phases in Dioleoylphosphatidylcholine/Oleic Acid and Dioleoylphosphatidylethanamine/Oleic Acid Binary Mixtures. *Langmuir* **2014**, *30*, 3337–3344.
- (24) Budin, I.; Szostak, J. W. Physical Effects Underlying the Transition from Primitive to Modern Cell Membranes. *Proc. Natl. Acad. Sci. U. S. A.* **2011**, *108*, 5249–5254.
- (25) Shirt-Ediss, B.; Ruiz-Mirazo, K.; Mavelli, F.; Solé, R. Modelling Lipid Competition Dynamics in Heterogeneous Protocell Populations. *Sci. Rep.* **2014**, *4*, 5675.
- (26) Haines, T. H. Anionic Lipid Headgroups as a Proton-Conducting Pathway along the Surface of Membranes: A Hypothesis. *Proc. Natl. Acad. Sci. U. S. A.* **1983**, *80*, 160–164.
- (27) Hauser, H.; Guyer, W.; Howell, K. Lateral Distribution of Negatively Charged Lipids in Lecithin Membranes. Clustering of Fatty Acids. *Biochemistry* **1979**, *18*, 3285–3291.
- (28) Markvoort, A. J.; Pfleger, N.; Staffhorst, R.; Hilbers, P. A.; van Santen, R. A.; Killian, J. A.; de Kruijff, B. Self-Reproduction of Fatty Acid Vesicles: A Combined Experimental and Simulation Study. *Biophys. J.* **2010**, *99*, 1520–1528.
- (29) Luisi, P. L.; Allegretti, M.; Souza, T.; Steiniger, F.; Fahr, A.; Stano, P. Spontaneous Protein Crowding in Liposomes: A New Vista for the Origin of Cellular Metabolism. *ChemBioChem* **2010**, *11*, 1989–1992.
- (30) Pereira de Souza, T.; Steiniger, F.; Stano, P.; Fahr, A.; Luisi, P. L. Spontaneous Crowding of Ribosomes and Proteins inside Vesicles: A Possible Mechanism for the Origin of Cell Metabolism. *ChemBioChem* **2011**, *12*, 2325–2330.
- (31) Stano, P.; D'Aguanno, E.; Bolz, J.; Fahr, A.; Luisi, P. L. A Remarkable Self-Organization Process as the Origin of Primitive Functional Cells. *Angew. Chem., Int. Ed.* **2013**, *52*, 13397–13400.
- (32) Cheng, Z.; Luisi, P. L. Coexistence and mutual competition of vesicles with different size distributions. *J. Phys. Chem. B* **2003**, *107*, 10940–10945.
- (33) Mavelli, F.; Ruiz-Mirazo, K. Theoretical Conditions for the Stationary Reproduction of Model Protocells. *Integr. Biol.* **2013**, *5*, 324–341.